An Investigation Into the Vehicle-Curved Bridge Dynamic Interaction

F. Javid[1], E. Esmailzadeh[2,*] and D. Younesian[3]

[1] MSc, [2] Professor, Faculty of Engineering and Applied Science, University of Ontario Inst. of Tech., Oshawa, Ontario, Canada.
[3] Associate Professor, School of Railway Engineering Iran University of Science and Technology, Tehran, Iran.

* Ezadeh@uoit.ca

Abstract

Moving vehicle dynamics is studied while travelling on a curved bridge in this paper. The vehicle including the driver and the passenger is simulated as a half-car planner model having six degrees of freedom, travelling on the bridge with constant velocity. The bridge is modeled as a curved beam that obeys the Timoshenko beam theory. Finite element method is employed to solve the combinational problem. The obtained numerical results are compared with those reported in the literature in a number of special cases. A parametric study is then carried out and effects of different parameters on both the vehicle and bridge dynamic behavior are investigated.

1. INTRODUCTION

The vehicle-bridge dynamic interaction has been centre of interests for last few decades. The interests arises by increasing the demand of using high-speed and heavy vehicles, which essentially lead to focused attention on the need for a better understanding of the dynamics of vehicle-bridge coupled systems. Basics and fundamentals of the dynamic analysis of different types of beams subjected to moving vehicles have been comprehensively addresses in two books provided by Fryba [1] and by Yang et al. [2]. The simplest approach to model a vehicle is to assume that the forces, due to the wheel-bridge interaction are constant; in other words, the beam is subjected to two moving constant loads. Although this approach considers the effects of two loads with the fixed distant on the beam, but it ignores the vehicle inertia and the vehicle-beam interaction, as well. Wen in 1960 improved that approach by considering the vehicle as a sprung mass with two axles. He investigated the typical uniform beam dynamic response while subjecting to the moving sprung mass. In fact, by considering the vehicle as a sprung mass with two axles, the effects of vehicle inertia and vehicle-beam interaction are considered along with the effects of the moving loads [1]. Fryba [1] improved Wen's model and formulated the differential equations of motion of a typical beam traversed by sprung masses with one, two and multi axles using d'Alembert's principle. The results for all three cases were compared and the

effects of a number of axles were investigated. More realistic dynamic condensation procedures proposed by Yang and Yau [3], which combine the separate vehicle and bridge models into a single coupled system in which all the original degrees of freedom are merged. Other methods, such as the mode superposition technique, have also been applied [4, 5] to study the dynamic response of multi-span beams subjected to moving loads. Esmailzadeh and Jalili [6] increased the vehicle degrees of freedom and considered the dynamics of the driver and passenger masses as well as their seats suspension systems. The presented vehicle model was a half-car planner model travelling along a simply supported Euler-Bernoulli beam. The beam dynamic response and the vehicle components bounce (tires, body, passenger, and driver) were observed. A nonlinear vehicle-bridge interaction model was developed by Kargarnovin et al. [7] to analyze the ride comfort quality of the high-speed trains travelling on the railway bridges. Surveying the literature shows that there are very few number of publications on the dynamics analysis of curved beams interacting with moving vehicles. Dynamic analysis of simply supported curved beams subjected to a single moving force has been carried out using the Galerkin's approach by Yang et al. [2]. Out-of-plane vibration of multi-span curved beams subjected to moving loads was analytically analyzed using the mode summation approach by Wang and Sang [8]. An accurate and effective solution for a circular curved beam subjected to a moving load was

proposed by Haung et al. [9] using the Laplace transform technique. The radial (in-plane) and out-plane bending-vibration responses of a uniform circular arch under the action of a moving load were investigated by Wu and Chiang [10-11] by means of the arch (curved beam) elements. Dynamic response of a slightly curved bridge under the action of a moving mass was studied by Reis and Pala [12] using an analytical approach. It is found that the dynamic interaction between a moving vehicle and a curved beam is still an open problem in the literature and needs to be further investigated. In this article, the vehicle-bridge interaction in extended for vehicles traveling on the curved bridges. The combinational problem is formulated by the Finite Element Method. In order to validate the result, a typical beam and vehicle properties are selected from the literature. The results are compared with the selected work, and it is shown that the presented results are in good agreement with those in the literature. Finally, a typical vehicle with 6 DOF is employed to simulate the moving vehicle on the curved beam. A parametric study is then carried out and effects of different parameters on the vehicle responses and bridge defections are investigated.

2. MATHEMATICAL MODELING AND VALIDATION

The major difference between curved beam and straight beam, which makes the study of the curved beams more complicated, is that the structural deformations in a curved beam depend on not only the rotation and radial displacement, but also the coupled tangential displacement caused by the curvature of structures.

The aim of this section is to develop the governing equation of the curved beam, as illustrated in Figure 1, with considering the effects of the shear deformation and rotary inertia. As discussed earlier the axial extensibility plays a major role in modeling the curved beam, hence, the effects of it will be included in the following formulations. Doing so, the extended Hamilton theory principal is applied to derive the governing differential equations of motion:

$$\int_{t_1}^{t_2} \delta(T - V)dt + \int_{t_1}^{t_2} \delta W_{nc} dt = 0 \qquad (1)$$

where the kinetic energy (T) and the potential

energy (V) can be expressed as:

$$T = \frac{1}{2}\int_L \rho A(s)\left(\frac{\partial w(s,t)}{\partial t}\right)^2 ds + \frac{1}{2}\int_L J(s)\left(\frac{\partial \psi(s,t)}{\partial t}\right)^2 ds$$
$$+ \frac{1}{2}\int_L \rho A(s)\left(\frac{\partial u(s,t)}{\partial t}\right)^2 d_s \qquad (2\text{-}a)$$

$$V = \frac{1}{2}\int_L EI(s)\left(\frac{\partial \psi(s,t)}{\partial s}\right)^2 ds + \frac{1}{2}\int_L k\,GA(s)\beta^2(s,t)ds +$$
$$\frac{1}{2}\int_L EA(s)\left(\frac{\partial u_T(s,t)}{\partial s}\right)^2 ds \qquad (2\text{-}b)$$

where

E   Young's elastic modulus
G   shear modulus
k   Timoshenko's shear coefficient
ρ mass per unit length
I(x)   area moment of inertia
J(x)   second moment of inertia
A(s)   cross-sectional area
w   beam radial transverse response
u   tangential displacement
β rotation due to shear deformation
ψ rotation due to bending

As it is provided in the equations, the axial extensibility $(du_T(s)/ds)$ is considered in the formulations. It should be noted that $\delta W_{nc} = 0$ since there is no external force acting on the beam.

By substituting the geometrical relationships into Equations (2), and applying the extended Hamilton's principle, the following three governing differential equations of motion can be obtained:
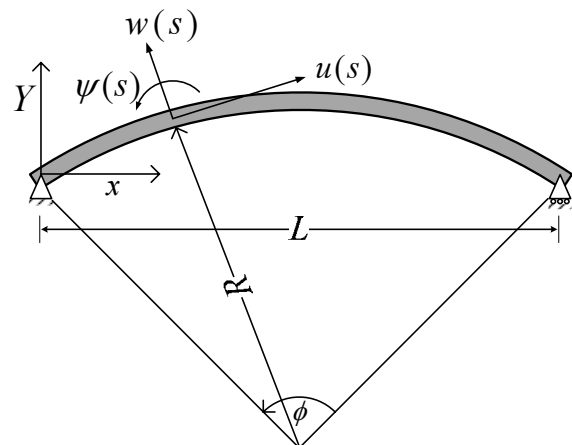

Fig. 1. Schematic diagram of curved beam with the defined coordinates

$$\rho A(s)\frac{\partial^2 w(s,t)}{\partial t^2} + \frac{\partial}{\partial s}\left[kGA(s)\left(\frac{\partial w(s,t)}{\partial s} - \frac{u(s,t)}{R} - \psi(s,t)\right)\right]$$ (3-a)

$$-\frac{EA(s)}{R}\left(\frac{\partial u(s,t)}{\partial s} + \frac{w(s,t)}{R}\right) = 0$$

$$\rho A(s)\frac{\partial^2 u(s,t)}{\partial t^2} + \frac{kGA(s)}{R}\left(\frac{\partial w(s,t)}{\partial s} - \frac{u(s,t)}{R} - \psi(s,t)\right)$$ (3-b)

$$+\frac{\partial}{\partial s}\left[EA(s)\left(\frac{\partial w(s,t)}{\partial s} + \frac{w(s,t)}{R}\right)\right] = 0$$

$$J(s)\frac{\partial^2 \psi(s,t)}{\partial t^2} + \frac{\partial}{\partial s}\left[EI(s)\left(\frac{\partial \psi(s,t)}{\partial s}\right)\right]$$ (3-c)

$$+kGA(s)\left(\frac{\partial w(s,t)}{\partial s} - \frac{u(s,t)}{R} - \psi(s,t)\right) = 0$$

where R indicates the beam curvature radius.

The geometrical properties of any circular curved beam can be defined by three parameters, namely, beam span length (L) beam curvature angle (ψ) beam curvature radius (R) which they are related to each other by the equation below:

$$R = \frac{L}{2\sin(\frac{\phi}{2})}$$ (4)

Based on the equation, one should identify at least two of these parameters in order to define a circular curved beam. For the present study, the beam span length is considered to be constant and the beam curvature to be variable. Therefore, the other parameter, beam curvature radius, will be calculated based on the input values for the span length (L)curvature angle (ψ) Figure 2 illustrates the relation between the three parameters by showing two different circular curved beams with the same span length and different curvature angle and radius.

The corresponding vector of the generalized coordinates is then given by

$$q = \{u_1, w_1, \psi_1, u_2, w_2, \psi_2, ..., u_N, w_N, \psi_N\}^T$$ (5)

in which, N denotes the number of total nodes. The consequent mass matrix and stiffness matrix are then obtained as [14]

$$M = \begin{bmatrix} M_{ww} & 0 & 0 \\ 0 & M_{uu} & 0 \\ 0 & 0 & M_{\psi\psi} \end{bmatrix}$$ (6)

$$K = \begin{bmatrix} K_{ww} & K_{wu} & K_{w\psi} \\ K_{uw} & K_{uu} & K_{u\psi} \\ K_{\psi w} & K_{\psi u} & M_{\psi\psi} \end{bmatrix}$$ (7)

in which,

$$M_{ww} = M_{uu} = \int_{-1}^{1} \gamma A(\eta)N(\eta)N(\eta)^T J(\eta)d\eta$$ (8)

$$M_{\psi\psi} = \int_{-1}^{1} \gamma IN(\eta)N(\eta)^T J(\eta)d\eta$$ (9)

$$K_{ww} = \int_{-1}^{1}\left[k\,GAB(\eta)B(\eta)^T J^{-1}(\eta) + \right.$$

$$\left. +\frac{EA}{R}N(\eta)N(\eta)^T J(\eta)\right]d\eta$$ (10)

$$K_{uu} = \int_{-1}^{1}\left[E\,AB(\eta)B(\eta)^T J^{-1}(\eta) + \right.$$

$$\left. +\frac{kGA}{R^2}N(\eta)N(\eta)^T J(\eta)\right]d\eta$$ (11)

$$K_{\psi\psi} = \int_{-1}^{1}\left[E\,IB(\eta)B(\eta)^T J^{-1}(\eta) + \right.$$

$$kGAN(\eta)N(\eta)^T J(\eta)\Big]d\eta$$ (12)

$$K_{uw} = \int_{-1}^{1} \left[\frac{EA}{R} N(\eta)^T B(\eta) J^{-1}(\eta) - \right.$$

$$\left. \frac{kGA}{R} B(\eta)^T N(\eta) \right] d\eta \qquad (13)$$

$$K_{w\psi} = -\int_{-1}^{1} \left[kGAB(\eta)^T N(\eta) \right] d\eta \qquad (14)$$

$$K_{u\psi} = -\int_{-1}^{1} \left[\frac{kGA}{R} N(\eta)^T N(\eta) J(\eta) \right] d\eta \qquad (15)$$

where, $B(\eta) = dN / d\eta$. The following governing equation of motions in the FE form can be then obtained:

$$[M_{3N \times 3N}]\{\ddot{q}_{3N \times 1}\} + [K_{3N \times 3N}]\{q_{3N \times 1}\} = \{f_{3N \times 1}(t)\} \qquad (16)$$

As illustrated in Figure 2 two different circular curved beams are drawn, S and S', between two points of A and B. Both share the same span length, but different curvature angle and radius. It can be seen that increasing the curvature angle makes the radius to decrease; however, the length of the curve will be increased (S > S').
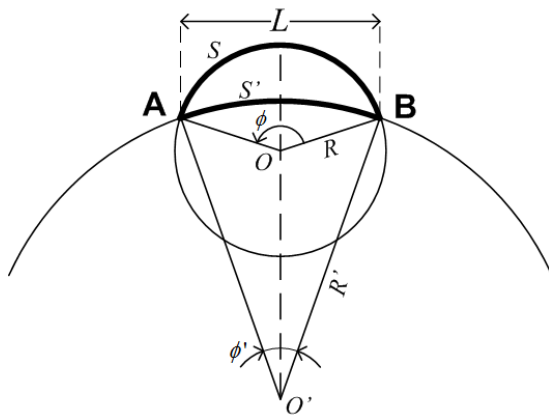
As discussed before, for this study the length is kept

Table 1. Properties of the curved beam [13]

Elastic modulus (E)	70 GPa
Shear modulus (G)	24.7 GPa
Density (ρ)	2777 kg/m^3
Cross-section area (A)	4 m^2
Second moment of area (I)	0.01 m^4
Shear coefficient (k)	5/6
Beam curvature radius (R)	0.75 m
Beam curvature angle (ϕ)	90°
R/r	15
l/r	23.56

constant, curvature angle is given, and the radius will be calculated. Timoshenko beam elements are employed to include the effects of shear deformation and rotary inertia. In order to generate the elastic circular curved beam, 100 straight Timoshenko beam segments are utilized, as described in Figure 3.

In order to validate the beam model, has a typical uniform circular curved beam is selected with the geometrical and physical properties listed in Table 1.

where r is the radius of gyration and is equal to $r = \sqrt{I/A}$.

The first ten natural frequencies of the uniform circular curved beam with the hinged-hinged boundary condition are obtained by the FEA. The natural frequencies are converted to non-dimensional form in order to compare the generated results with those available in the literature [13-14] as provided in Table 2. It can be realized that very close agreement between the presented results and those reported in the literature.

Fig. 2. The relation between circular curved beam parameters
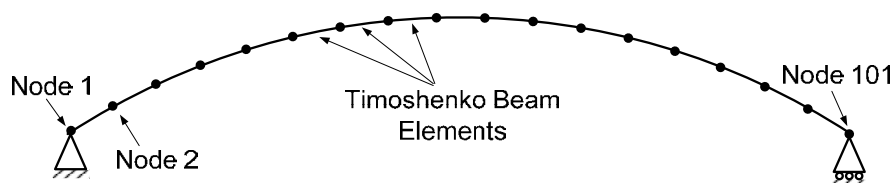
Fig. 3. Curved beam modeling in FEM

Table 2. Non-dimensional frequencies $\lambda = \omega l^2 \sqrt{\rho A/EI}$ of the curved beam with hinged-hinged boundary condition

Mode	Ref. [13]	Ref. [14]	Present Study
1	29.61	29.280	29.2627
2	33.01	33.305	33.2983
3	67.24	67.124	67.0724
4	79.6	79.971	79.9582
5	107.7	107.851	107.7653
6	144.5	14 .618	143.5 35
7	155.2	156.666	156.6343
8	191.3	190.477	190.3772
9	223.7	225.361	225.4156
10	235.3	234.524	234.4843

3. NUMERICAL RESULTS AND DISCUSSION

The aim of this section is to create a moving half-car model on the curved Timoshenko beam, showed in Figure 4. The curved beam is modeled using a sequence of straight beam elements, which has been proven to be acceptable in the literature.
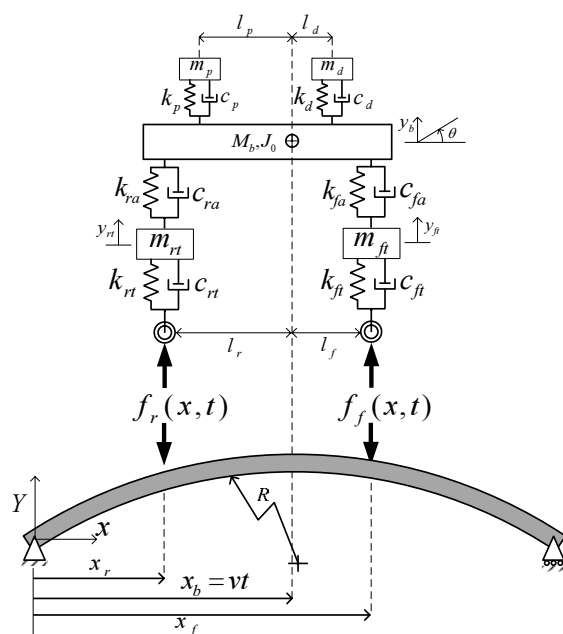
A proper input table is utilized to constraint the vehicle movement along the beam as $x_b = v t$ in order to ensure the velocity of the vehicle along the beam would remains constant, where v is the vehicle constant speed and t is time with the origin of the moment when the first wheel arrives on the beam.

As an especial case, the straight beams act as the curved beams with an infinite curvature radius. The aim of this section is to generate a moving half-car planner model on a straight Timoshenko beam. The selected vehicle model is half-car planner model with six degrees of freedom, illustrated in Figure 5.

A typical Timoshenko beam and half-vehicle planner model are selected from literature to validate the presented method and modeling. Esmailzadeh and Jalili [6] presented the analytical solution for a thin beam traversed by a moving vehicle. Table 3 provides the beam properties. As mentioned in the introduction, Esmailzadeh and Jalili investigated the problem of Euler-Bernoulli beam traversed by a moving vehicle; however, the Timoshenko beam theory is employed in this study. Therefore, to ensure the validity of the generated results by present finite element method, all Timoshenko elements in the model are substituted with Euler-Bernoulli beam elements for this section.

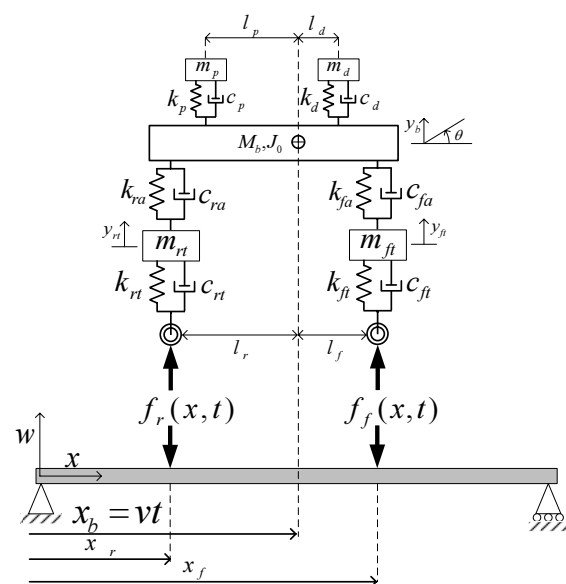The geometrical and mechanical of the vehicle model presented by Esmailzadeh and Jalili. [6] which

Fig. 4. Timoshenko curved beam traversed by moving vehicle [15]

Fig. 5. The moving vehicle on a suspension bridge. Beam force interaction with a six DOF half-car planner model [6].

Table 3. Properties of the beam [6]

Elastic modulus	207 GPa
Mass per unit length	20 000 kg/m
Cross-sectional area	4.94 m^2
Second moment of area	0.174 m^4
Beam viscous damping	1750 N.s/m
Beam length	100 m

is a six DOF half-car planner model, as illustrated in Figure 4, are listed in Table 4.

Figure 6 presents the history diagrams of the driver vertical motion (bounce), the passenger, the vehicle body, the front tire and the rear tire bounce for the vehicle speed of $v=88km/h$(24.44 m/s). The figure

also compares the generated result using the presented method with those obtained by Esmailzadeh and Jalili [6].

As it is presented in Figure 5, the obtained results are in good agreement with those obtained with Esmailzadeh and Jalili [6]. The major difference between two result sets occurs when the vehicle passes the beam midpoint and the sheer force changes rapidly from the positive maximum to its negative minimum. The rapid change in the sheer force cannot be captured by all the elements of the beam; therefore, the slight difference between the generated results and those obtained by Esmailzadeh and Jalili [6] is observed.

It is shown that the maximum deflection (bounce) of the vehicle components do not occur when the vehicle passes the midpoint. The reason is that the beam maximum deflection does not occur when the
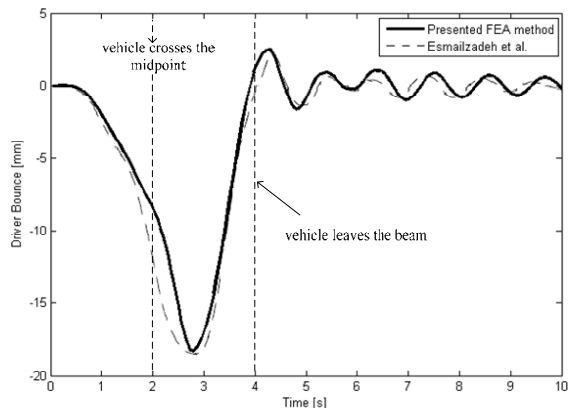
Table 4. Mechanical properties of the vehicle [6]

Body mass (M_b)	1794.4 kg
Body rotational mass moment of inertia (J_0)	443.05 kg.m^2
Front axle mass (m_{ft})	87.15 kg
Rear axle mass (m_{rt})	140.4 kg
Driver mass (m_d)	75 kg
Passenger mass (m_p)	75 kg
Front axle damping ratio (c_{fa})	1 190 N.s/m
Rear axle damping ratio (c_{ra})	1 000 N.s/m
Front tire damping ratio (c_{ft})	14.6 N.s/m
Rear tire damping ratio (c_{rt})	14.6 N.s/m
Driver seat damping ratio (c_d)	62.1 N.s/m
Passenger seat damping ration (c_p)	62.1 N.s/m
Front axle stiffness (k_{fa})	66 824.4 N/m
Rear axle stiffness (k_{ra})	18 615.0 N/m
Front tire stiffness (k_{ft})	101 115.0 N/m
Rear tire stiffness (k_{rt})	101 115.0 N/m
Driver seat stiffness (k_d)	14 000.0 N/m
Passenger seat stiffness (k_p)	14 000.0 N/m
Distance form front wheel to body C.G.(l_f)	1.271 m
Distance form rear wheel to body C.G.(l_r)	1.716 m
Distance form driver seat to body C.G.(b_d)	0.481 m
Distance form driver seat to body C.G.(b_p)	1.313 m

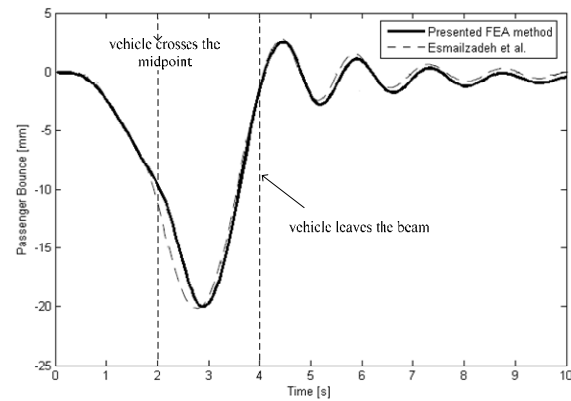**Fig. 6(a).** Time history diagram of the driver seat

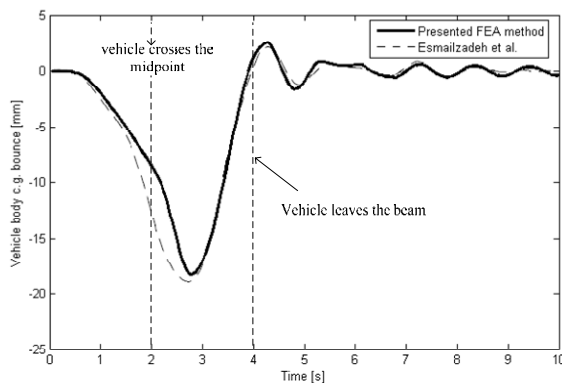**Fig. 6(b).** Time history diagram of the passenger seat

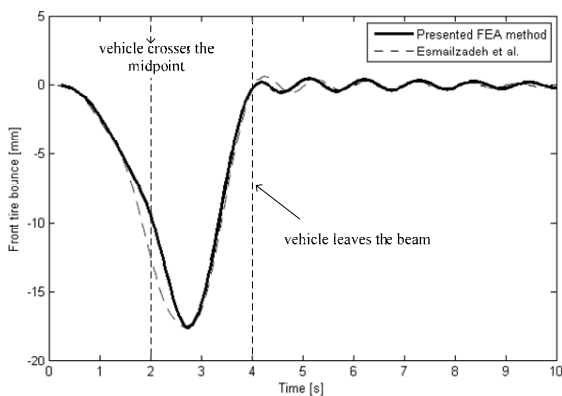**Fig. 6(c).** Time history diagram of the vehicle body

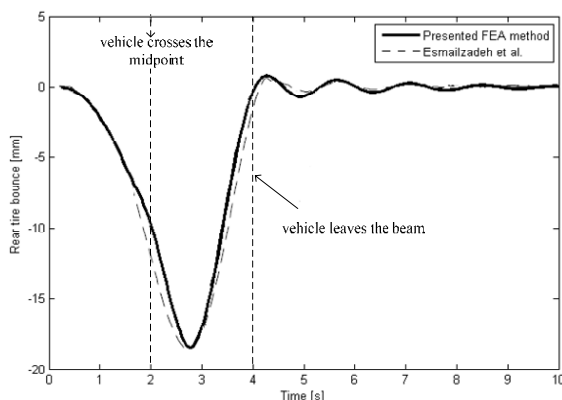**Fig. 6(d).** Time history diagram of the front tire

Fig. 6(e). Time history diagram of the rear tire

Fig. 6. Time history diagram of the driver , the passenger, the vehicle body, the front tire and the rear tire bounce for the vehicle speed of $v=88km/h$(24.44 m/s).

vehicle locates on the mid-span. It should be mentioned that the beam deflection magnitude is relatively larger than those for the vehicle

components.

To study the effects of the bridge curvature on the vehicle dynamics, the same bridge and vehicle model are employed, but the curvature is added to the bridge, as presented in Table 5. The geometrical and mechanical of the selected vehicle model are listed in Table 4 and the vehicle speed is assumed to be *10 m/s*.

Table 5. Properties of Timoshenko beam with curvature angle [15]

Elastic modulus	207 GPa
Mass per unit length	20 000 kg/m
Cross-sectional area	4.94 m^2
Second moment of area	0.174 m^4
Beam viscous damping	1750 N.s/m
Shear coefficient	5/6
Beam length	100 m
Beam curvature angle	60°

Figure 7 illustrates the history diagram of the driver vertical motion (bounce), the passenger, the vehicle body, the front tire and the rear tire bounce. To understand the vehicle dynamics, the deflection of the vehicle components, i.e. vehicle body, tires, and seats, are studied in two different approaches. Doing so, two functions are defined, namely absolute and relative as presented below:

$$Deflection_{abs} = y_c(t)$$

$$Deflection_{rel} = y_c(t) - w(vt, t)$$

(5)

where $y_c(t)$ is the deflection of the component and $w(vt,t)$ is the beam deflection at the location of the vehicle.

It should be noted that the vehicle leaves the bridge after 5 sec, though it continues the movement after the bridge to achieve better understanding of its dynamics. As it is illustrated in Figure 7, there are some similarities in all the presented graphs such as: The absolute function and relative function match together
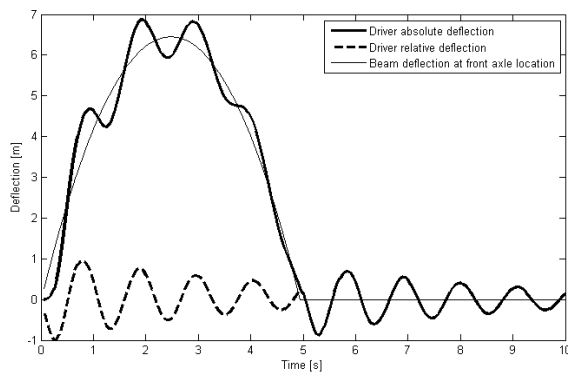
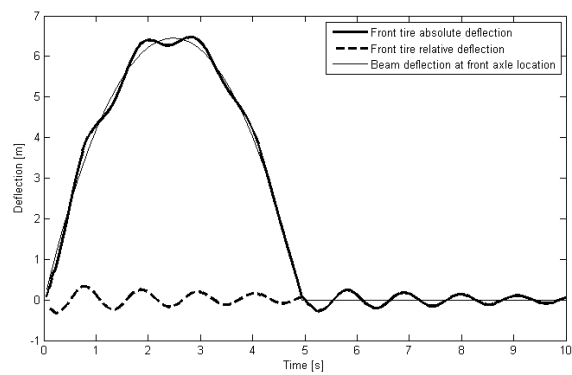**Fig. 7(a).** Time history diagram of the driver
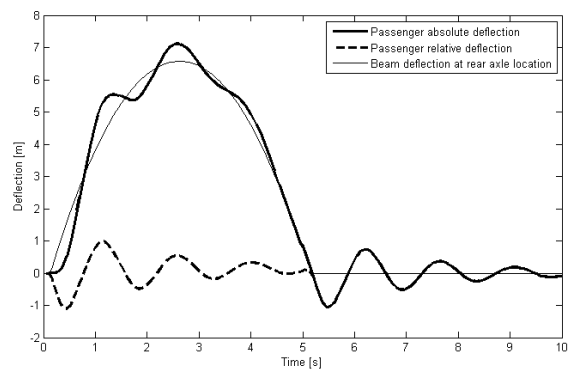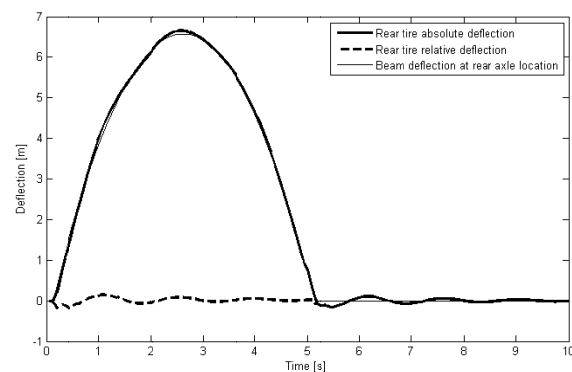
Fig. 7(b). Time history diagram of the passenger

Fig. 7(c). Time history diagram of the vehicle body

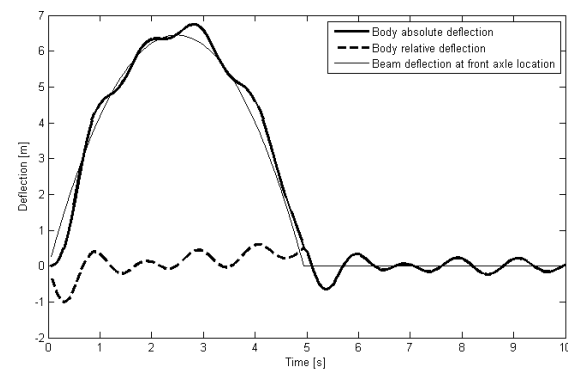**Fig. 7(d).** Time history diagram of the front tire

Fig. 7(e). Time history diagram of the rear tire

Fig. 7. Time history diagram of (a) the driver , (b) the passenger, (c) the vehicle body, (d) the front tire and (e) the rear tire bounce for the vehicle speed of
$v=88km/h$(24.44 m/s).

the first stage, the vehicle components face the rapid changes of the base altitude due to the curved beam geometry, which makes them to oscillate. However, the oscillations decrease because of the dampers.

4. CONCLUSION

The vehicle-structure interaction problem of a curved bridge traversed by a moving vehicle was investigated. The vehicle including the occupants was modelled as a half-car planar model with six degrees-of-freedom, and the bridge was assumed as a Timoshenko beam. Comparing the time history diagram of the moving vehicle on the straight bridge with those obtained on the curved bridge. It was found that the front passenger feels larger relative and absolute accelerations in case of the curved bridge.

when the vehicle leaves the beam; however, there are significant differences between them when the vehicle is on the beam. The relative deflections of all the vehicle components have two stages: while the vehicle is on the beam, when the vehicle leaves the beam. In

While the order of magnitude of acceleration remains unchanged for rear and front passengers in case of the straight bridge. It was also observed that the passenger's displacement almost follow the bridge deflection pattern in case of the straight bridges. But a significant difference between these two values was observed when the vehicle is travelling on the curved bridge.

REFERENCES

1. Fryba, L. (1999) Vibration of Solid and Structures under Moving Loads, Prague: Telford Books.
2. Yang, Y.B., Yau, J.D., Wu, S.U., (2004) Vehicle-Bridge Interaction Dynamics, World Scientific Publishing.
3. Yang, Y.B. and Yau J.D. (1997), 'Vehicle-bridge interaction element for dynamic analysis', Journal of Structural Engineering, 123 (11): 1512-18
4. Henchi, K., Fafard, M., Dhatt, G. and Talbot, M. (1997), 'Dynamic behaviour of multi-span beams under moving loads', Journal of Sound and Vibration, 199 (1): 33-50.
5. Wang, R.T. (1997), 'Vibration of multi-span Timoshenko beams to a moving force', Journal of Sound and Vibration, 207 (5): 731-42
6. Esmailzadeh, E., Jalili, N. (2003) 'Vehicle-passenger-structure interaction of uniform bridges traversed by moving vehicles', Journal of Sound and Vibration 260(4): 611-635.
7. Kargarnovin, M.H., Younesian, D., Thompson, D.J., Jones, C.J.C., (2005), 'Ride Comfort of High-Speed Trains Travelling over Railway Bridges', Vehicle System Dynamics, 43(3): 173-197.
8. Wang, R.-T., Sang, Y.-L. (1999) 'Out-of-plane vibration of multi-span curved beam due to moving loads', Structural Engineering and Mechanics 7 (4): 361-375.
9. Huang, C.S., Tseng, Y.P., Hung, C.L., (2000), 'An accurate solution for the responses of circular curved beams subjected to a moving load', International Journal for Numerical Methods in Engineering 48(12): 1723-1740.
10. Wu. J-S., Chiang L.-K., (2003), 'Out-of-plane responses of a circular curved Timoshenko beam due to a moving load', International Journal of Solids and Structures 40(26): 7425-7448.
11. Wu. J-S., Chiang L.-K., (2004), 'Dynamic analysis of an arch due to a moving load', Journal of Sound and Vibration, 268: 511–534.
12. Reis, M., Pala, Y. (2009) Dynamic Response of a Slightly Curved Bridges Under Moving Mass Loads, The Baltic Journal of Road and Bridge Engineering, 4(3): 143-148.
13. Eisenberger, M. and Efraim, E. (2001) 'In-plane vibrations of shear deformable curved beams', International Journal for Numerical Methods in Engineering, 52: 1221–1234.
14. Yang, F., Sedaghati, R. and Esmailzadeh, E. (2008) 'Free in-plane vibration of general curved beams using finite element method', Journal of Sound and Vibration 318: 850-867.
15. Javid, F., (2011), 'Vibration Suppression of Straight and Curved Beams Traversed by Moving Loads', M.Sc Dissertation, University of Ontario Institute of Technology.